PAPER H

REAL DATA EXAMPLES OF CROSS-WELL CLP ORTHOGONAL REFLECTION GATHERS

Nicholas Smalley and Jerry M. Harris

ABSTRACT

A new cross-well reflection imaging technique (Smalley, 1992) is applied to real data. The new orthogonal cross-well reflection gathers show moveout curves that are expected by the theory. Also shown in this paper is a cross-well reflection image using a series of constant velocity stacks, with the velocities estimated from the tomogram.

INTRODUCTION

There has recently been a lot of work on cross-well reflection imaging (Lazaratos, 1991, 1992). These results had some excellent cross-well reflection images. This initial work in cross-well reflection imaging encouraged a development of a new theory for cross-well reflection imaging (Smalley, 1992). This new method developed a parallel between cross-well and surface seismic reflection stacking and imaging by creating a cross-well CLP (Common Lateral Point) stacking coordinate system (Smalley, 1992). This new method has the advantage over VSP - CDP mapping in that it provides both a framework for velocity analysis by derived moveout equations for orthogonal gathers, and gives us many different ways to look at the data by breaking the correction into two steps (HNMO and VLMO) as well as having two orthogonal gathers.

REAL DATA CROSS-WELL CDP GATHERS

After the cross-well data has been pre-processed for reflections we can immediately sort the data into the CLP coordinate gathers. The cross-well CLP polar coordinate system is parameterized by reflection depth. In the real data case we are examining here, we choose a reflection depth of 3000ft. The polar coordinates (α(Zr), r(Zr)) were then

computed based on this reflector depth. The data come from a West Texas cross-well survey; using upgoing reflections Figure 1 shows a theoretical CLP gather, which is where the coordinate $\alpha(Zr)$ is held constant. This is equivalent to a common ratio gather (Smalley, 1992). We see that the moveout is hyperbolic. The real data example shows this same moveout (Figure R1). The lateral point used is the midpoint between the wells; $\alpha=\pi/4$. If we hold r(Zr) constant, this is defined as a CRD (common radial distance) gather (Figure 2). We see that the moveout is a half period of a sine wave when it is plotted versus time squared. The real data shows this same moveout (Figure R2). However, the sine wave shape shown in the real data example has a moveout of the square root of a sine wave since it shown as a function of time. Therefore the moveout is not as prominent. The radial distance was binned between 28 and 32 feet.

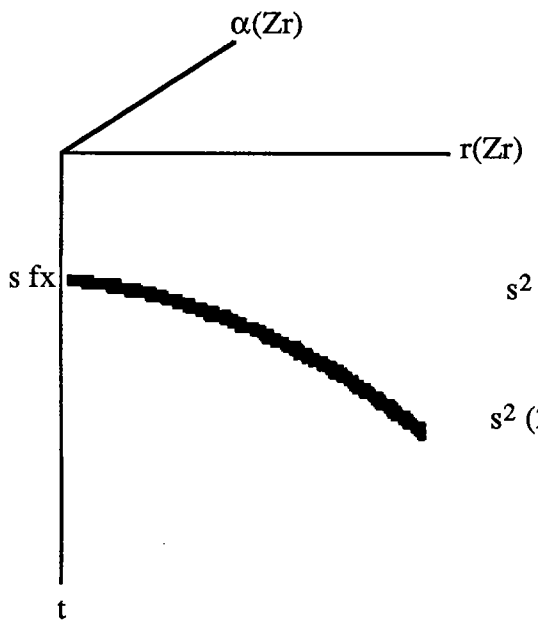

Figure 1. CLP gather.

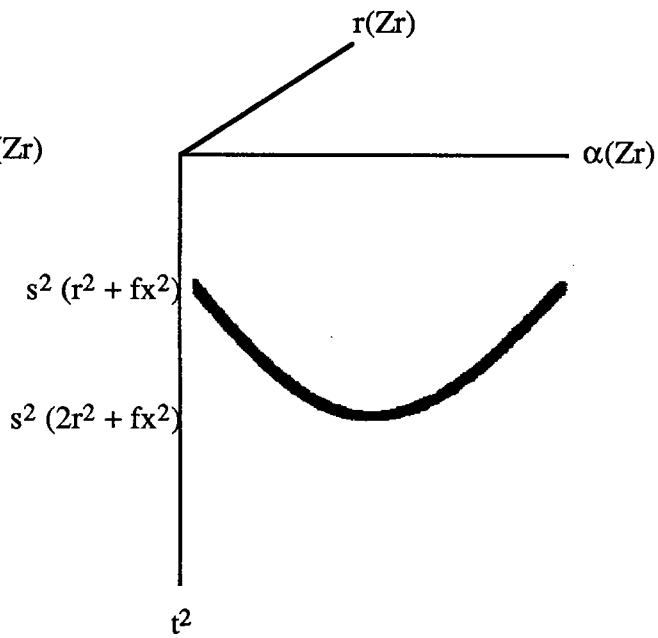

Figure 2. CRD gather.

The first step in correcting for the offset of the sources and geophones is the HNMO correction (Smalley, 1992). This is a correction for the horizontal offset of the wells. Figure 3 shows the CLP gather after the HNMO correction (CLP - HNMO gather). The moveout is now a sloped line that intersects the origin. Figure R3 shows the real data CLP - HNMO gather. Let us consider the prominent reflection near the top of the gather.

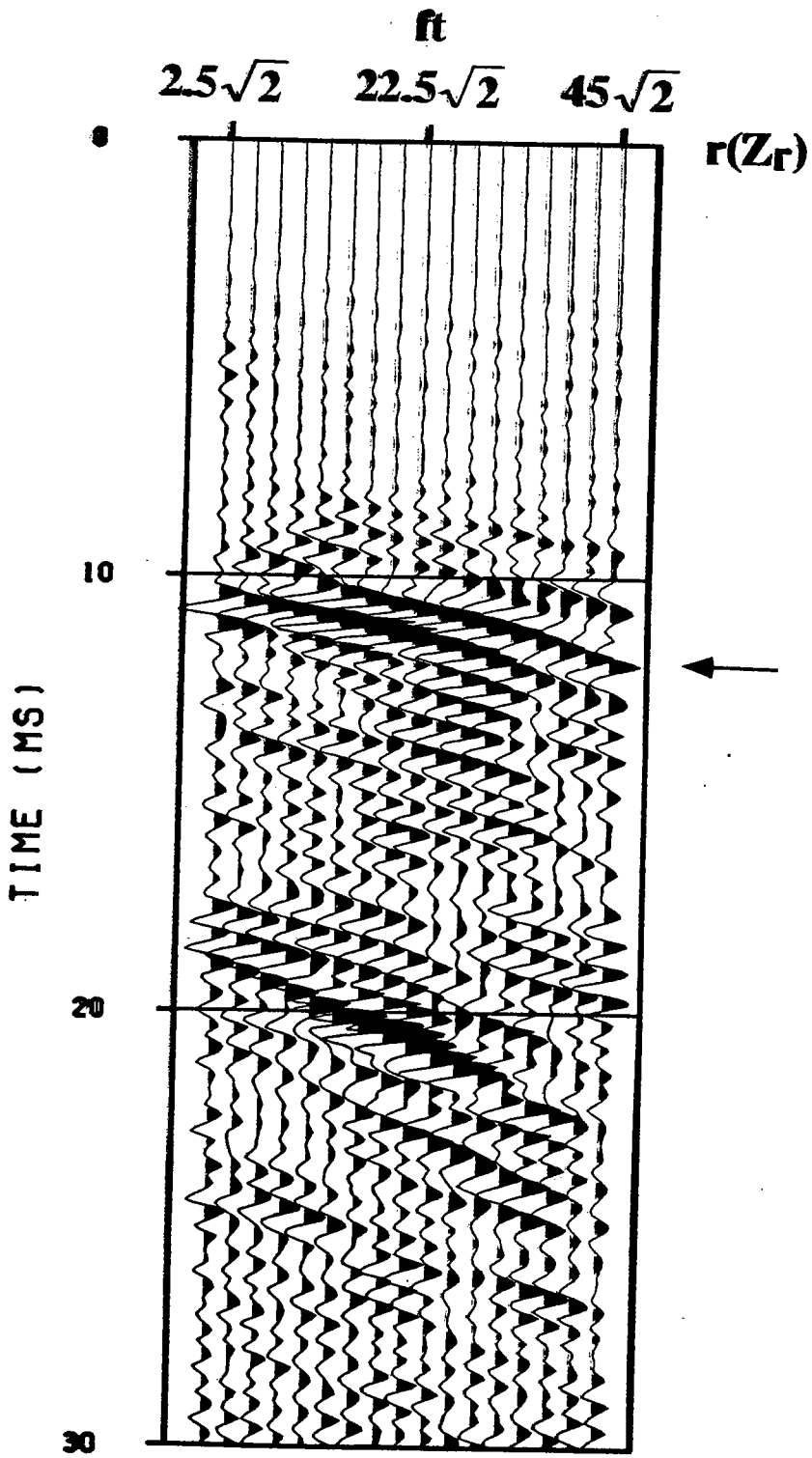

Figure R1. Real data CLP gather. The arrow shows the reflection event being examined.

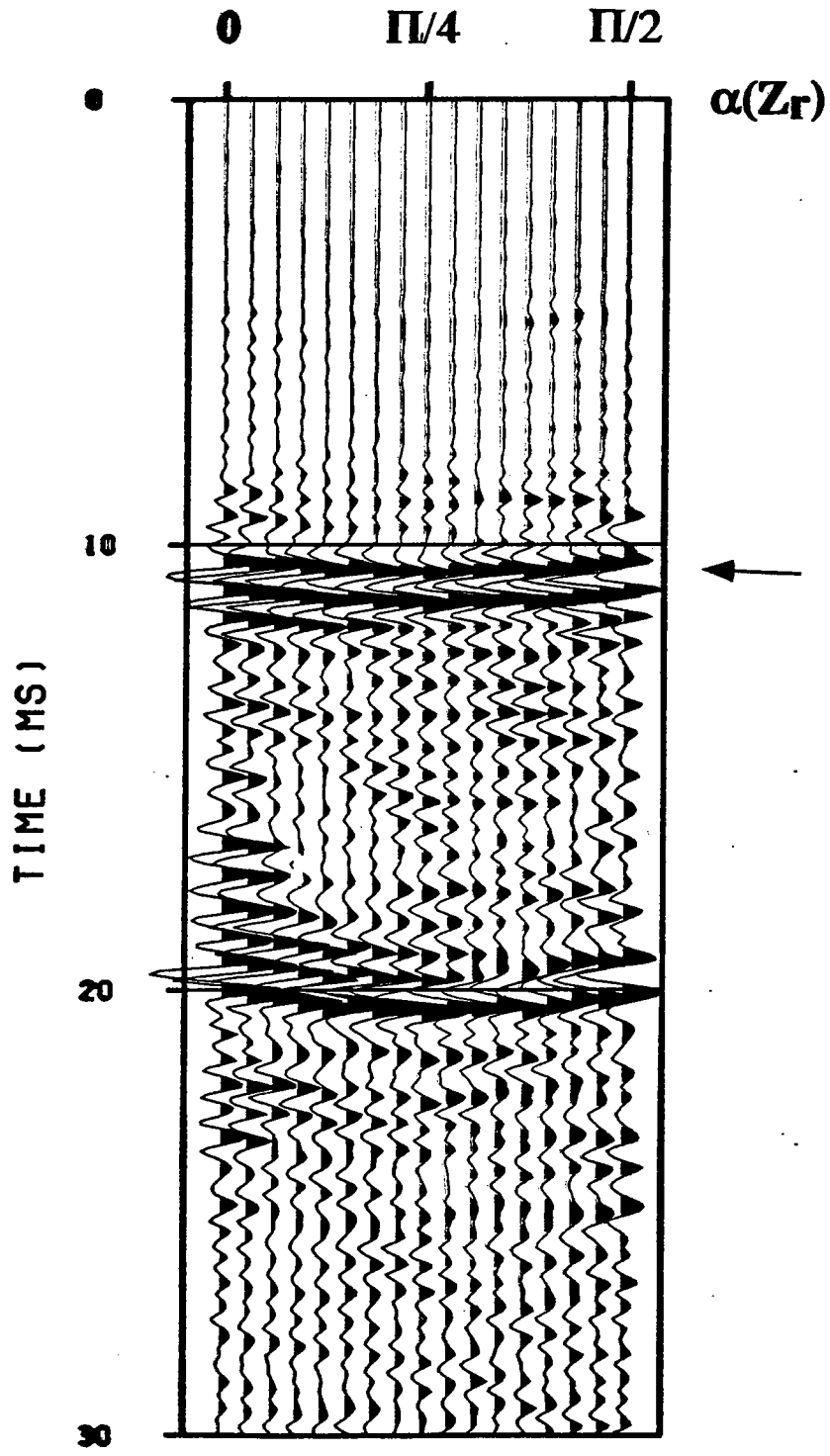

Figure R2. Real data CRD gather. The arrow shows the reflection event being examined.

The reflection moveout has a more linear moveout and has moved toward the origin. However it still has some residual hyperbolic moveout, and has an intercept on the time axis beneath the origin. This is because the reflection is deeper than the assumed reflector depth of 3000 feet. More discussion on this problem is detailed in another paper in this volume (Smalley, 1993). This gather also shows a stretch at small radial distances. The small radial distances correspond to wide angles of incidence. Figure 4 shows the CRD gather after the HNMO correction (CRD - HNMO gather). The moveout is still a half period sine wave that has moved up in time. Figure R4 shows the real data example of the CRD - HNMO gather.

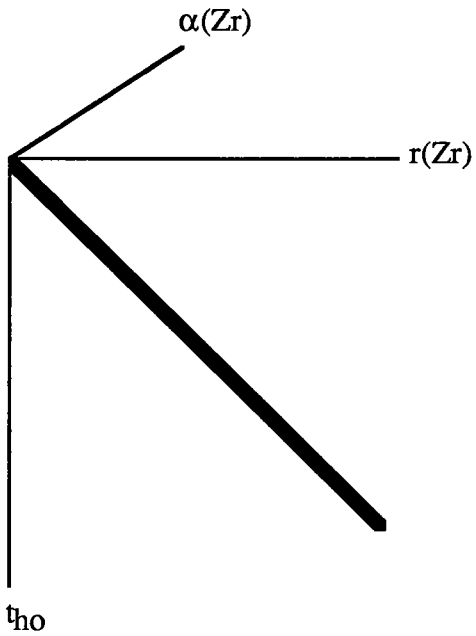

Figure 3. CLP - HNMO gather.

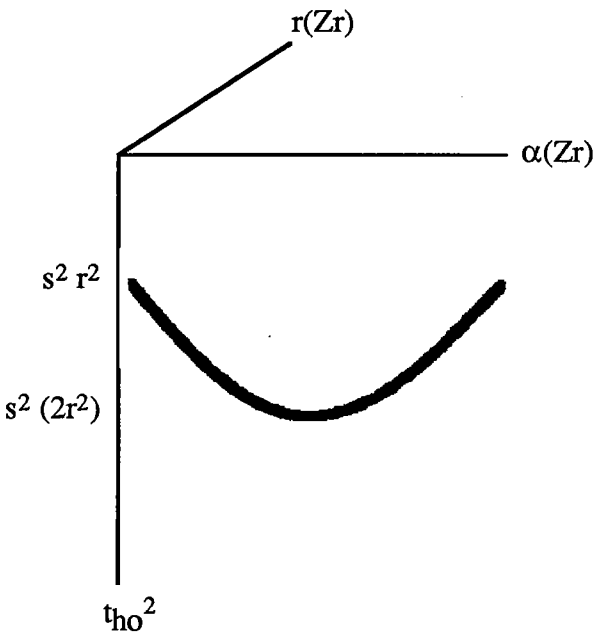

Figure 4. CRD- HNMO gather.

The next step in correcting for source - geophone offset is the VLMO correction (Smalley, 1992). This is a correction for the depths of the sources and geophones. Figure 5 shows the CLP gather after the VLMO correction (CLP - VLMO gather) which follows the HNMO correction. This flattens the event. The real data example in figure R5 also shows a flattened event, but with some residual slope. This is due to using a constant velocity estimated from the tomogram. Figure 6 shows the CRD gather after the VLMO correction (CRD - VLMO gather). This domain also yields a flat reflection. This gather is a pre-stack image of the reflection. The real data example in figure R6 shows a

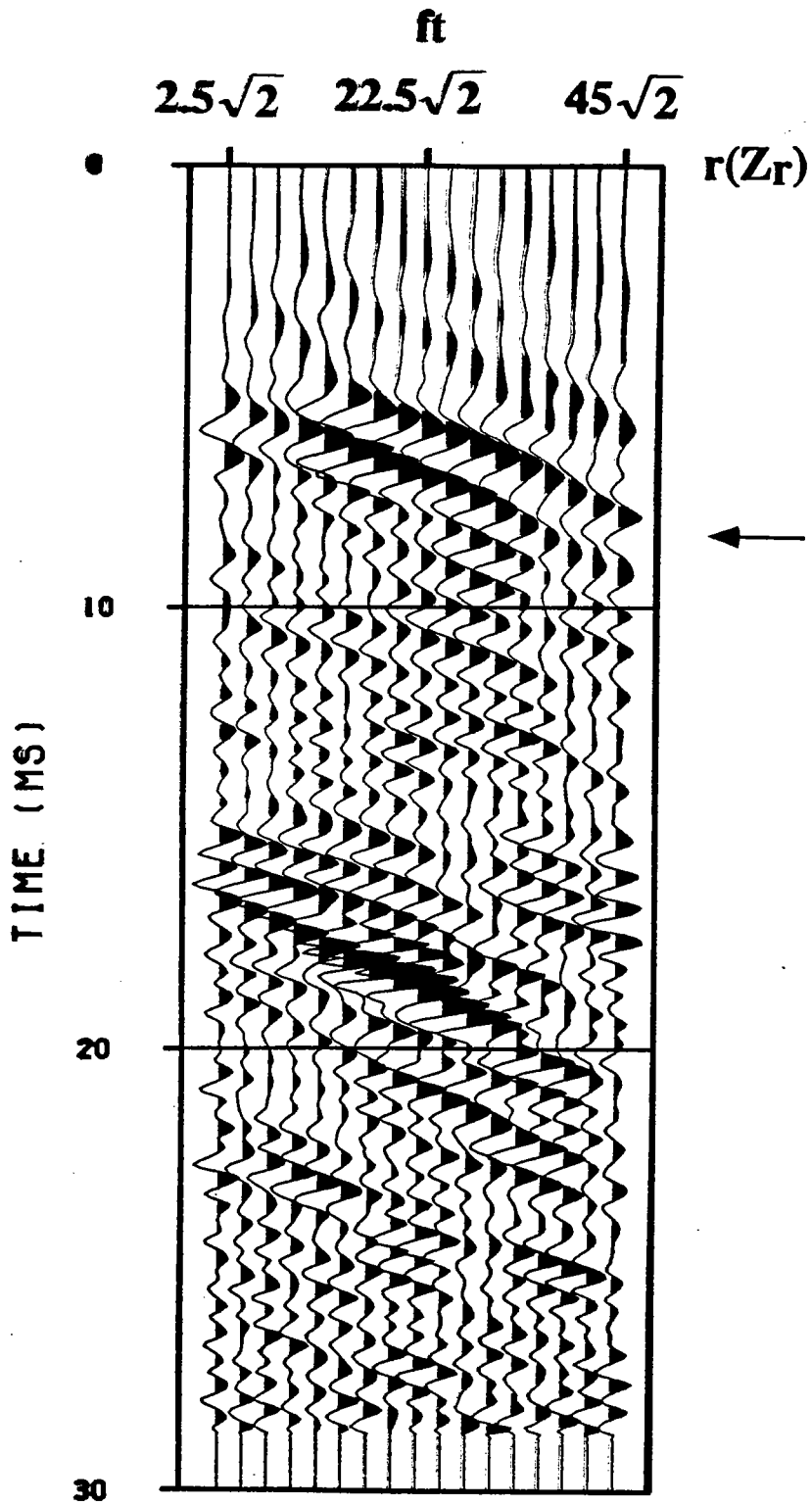

Figure R3. Real data CLP - HNMO gather.

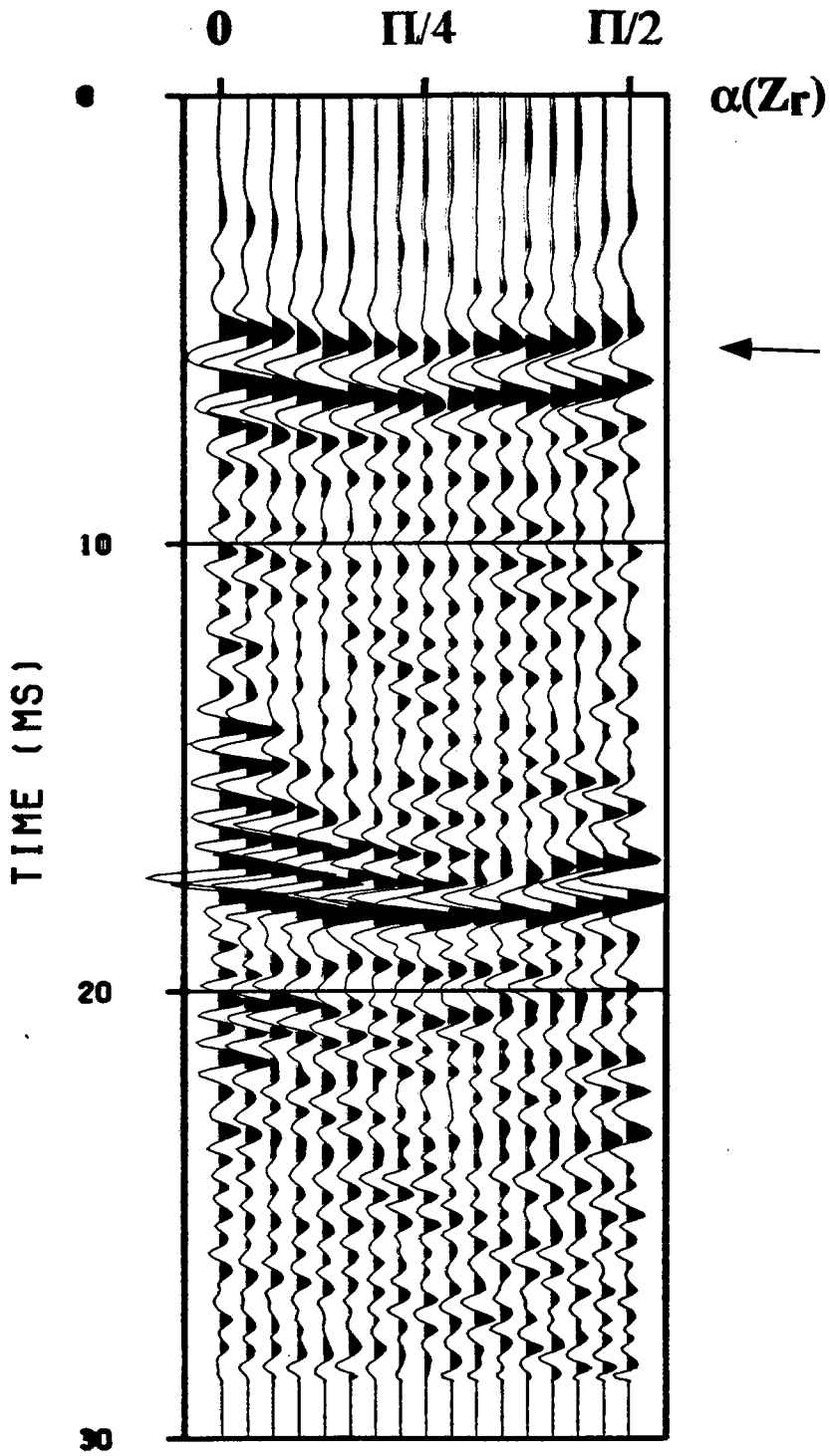

Figure R4. Real data CRD - HNMO gather.

coherent flat reflection. Figure 7 shows the event after stacking over r(Zr). This process parallels the surface seismic stack over h. Figure R7 shows the real data example of the stack. The reflection event has been enhanced.

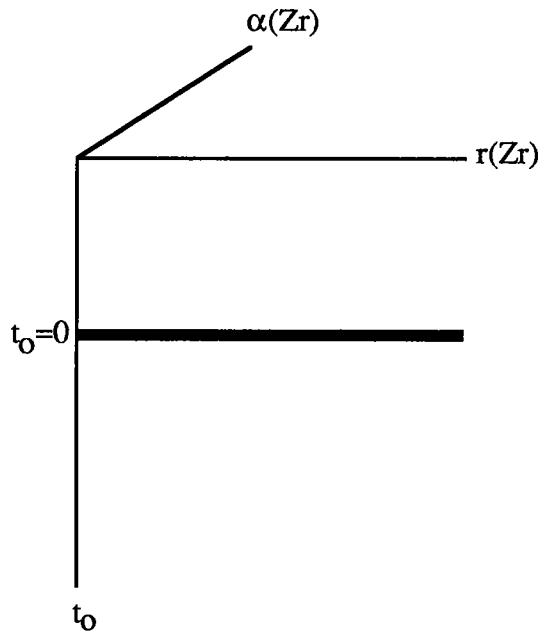

Figure 5. CLP - VLMO gather.

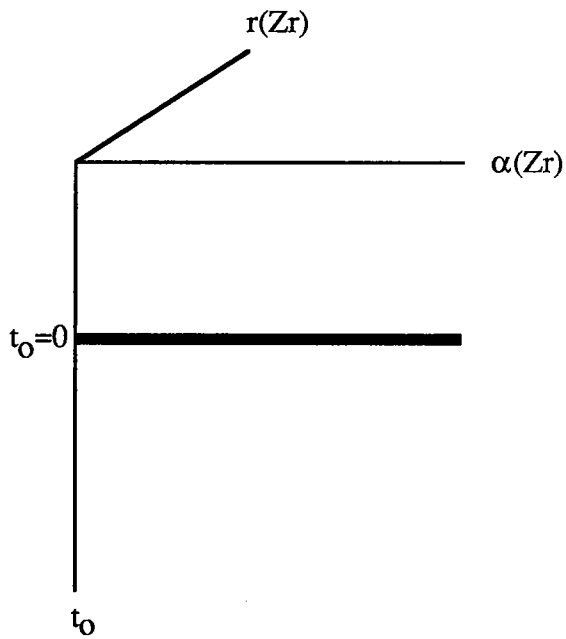

Figure 6. CRD - VLMO gather.

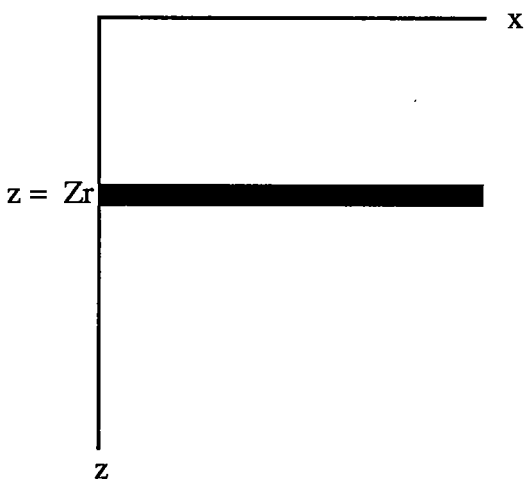

Figure 7. Stack over r(Zr), convert to x (space), convert to depth.

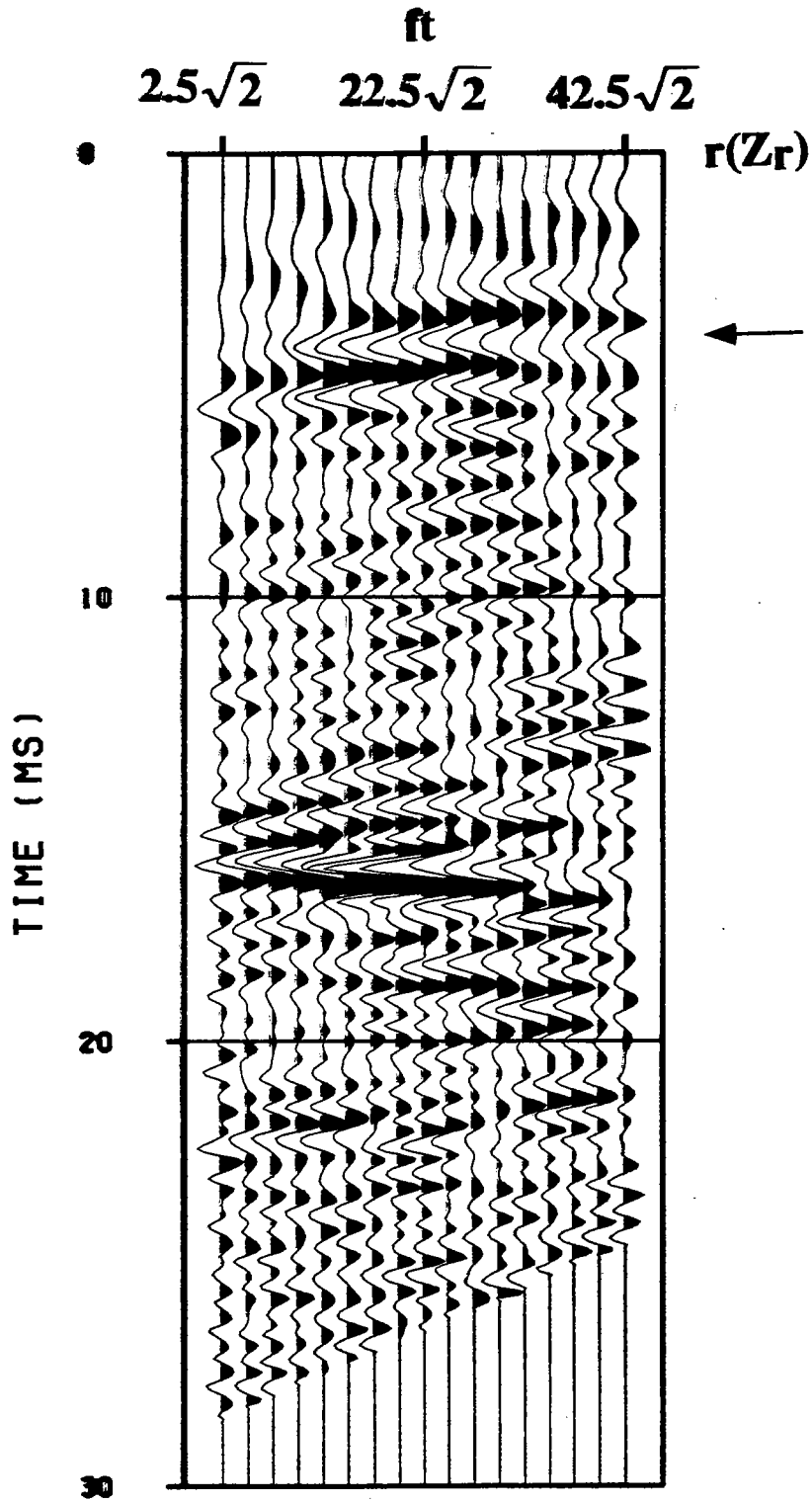

Figure R5. Real data CLP - VLMO gather.

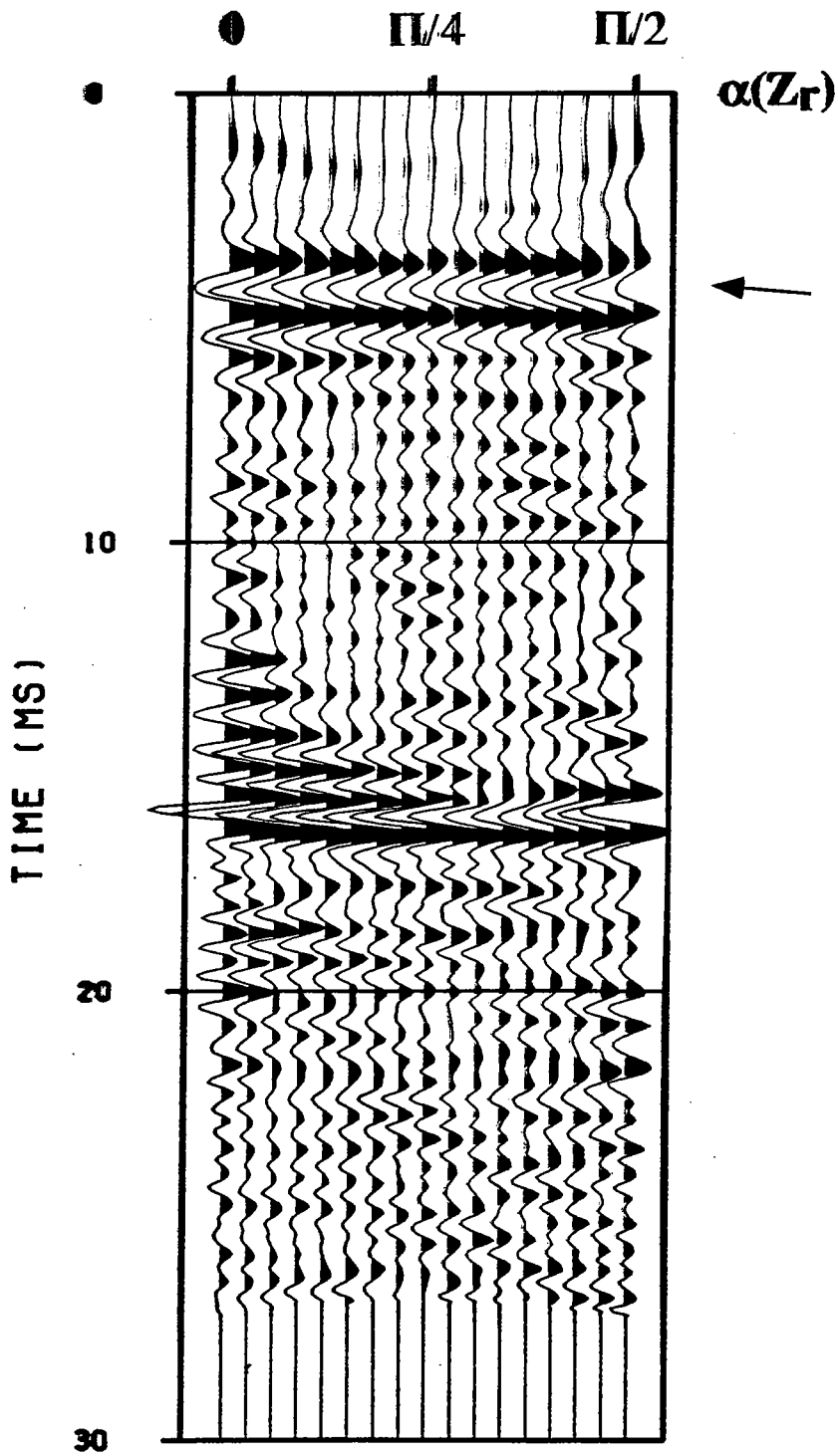

Figure R6. Real data CRD - VLMO gather.

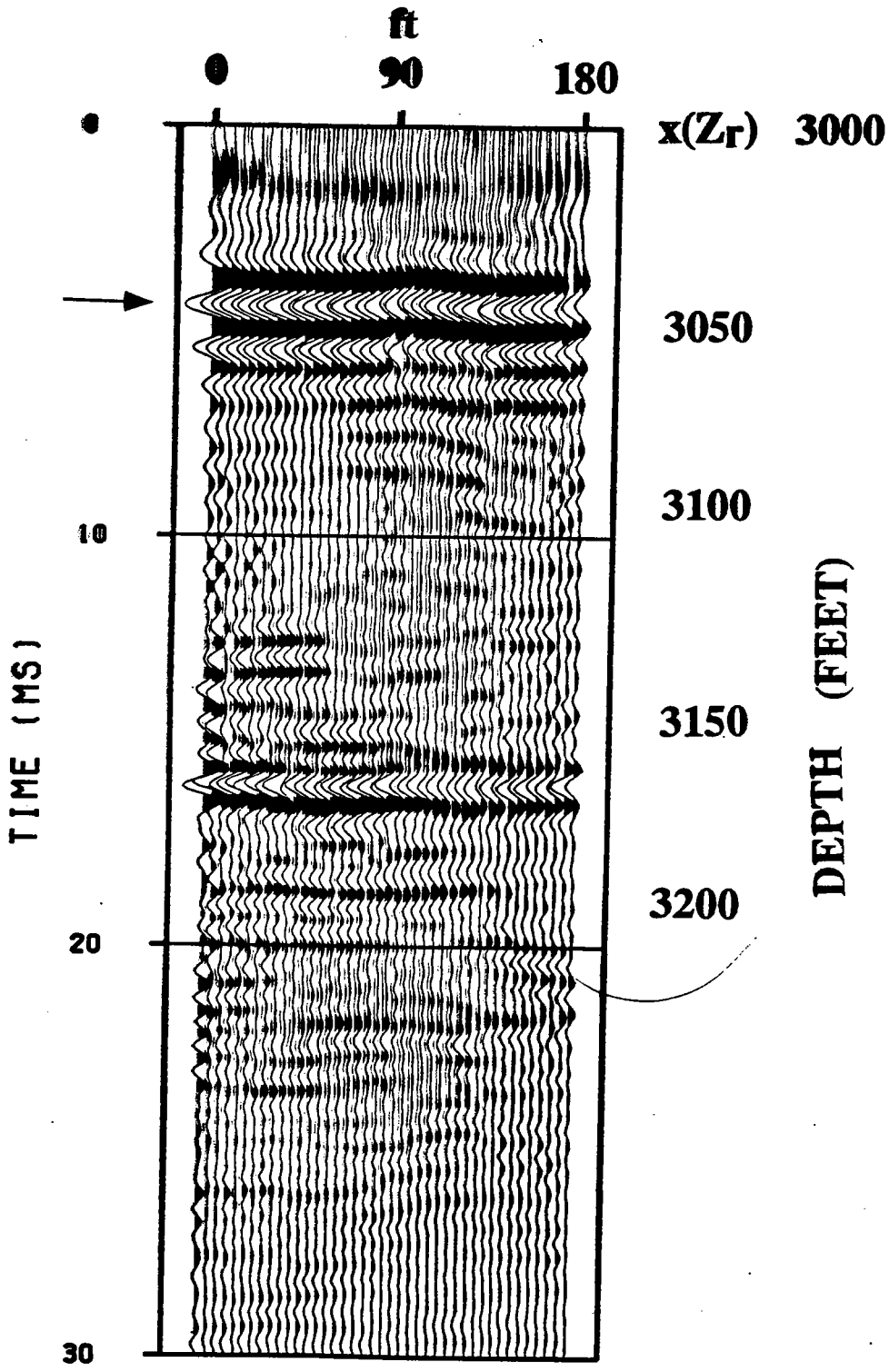

Figure R7. Stacked image.

COMPOSITE IMAGE

A composite image of the West Texas data set was completed using the imaging procedure previously described for several different assumed reflector depths using an increment of 50 ft, and constant velocities estimated from the tomogram (Figure R8). The same image with an AGC filter of 3 ms is shown in figure R9. We can see several reflection events. However the 50 ft increment between assumed reflector depths leads to errors in the CLP polar coordinate calculations, as well as losing a portion of the image towards the wells. Also the use of constant velocities estimated from the tomogram is not accurate enough to enhance the weaker reflections. These problems are both addressed in another paper in this volume (Smalley, 1993).

CONCLUSIONS

In this paper we have seen real data examples of the previously derived cross-well reflection CLP orthogonal gathers (Smalley, 1992). The moveouts of the individual gathers were consistent with the theoretically expected moveout curves. This is very important for further work using this system of reflection imaging. Another paper in this volume uses these moveout curves to obtain stacking velocities or slownesses for reflection imaging (Smalley, 1993). The composite reflection images also show that it is possible to image reflections by this method.

REFERENCES

Lazaratos, S., Rector, J.W., Harris, J.M., and Van Schaack, M., 1991, High Resolution Imaging with Cross-Well Reflection Data: STP vol. 2 Paper A.

Lazaratos, S., Rector, J.W., Harris, J.M., and Van Schaack, M., 1992, High Resolution Imaging of a West Texas Carbonate Reservoir: STP vol. 3 No. 1 Paper E.

Smalley, N., 1992, Cross-well Pre-Stack Partial Migration (Theory): STP vol. 3 No.1, Paper M.

Smalley, N., 1993, Cross-well Reflection Velocity Analysis: STP vol. 4 No.1, Paper G.

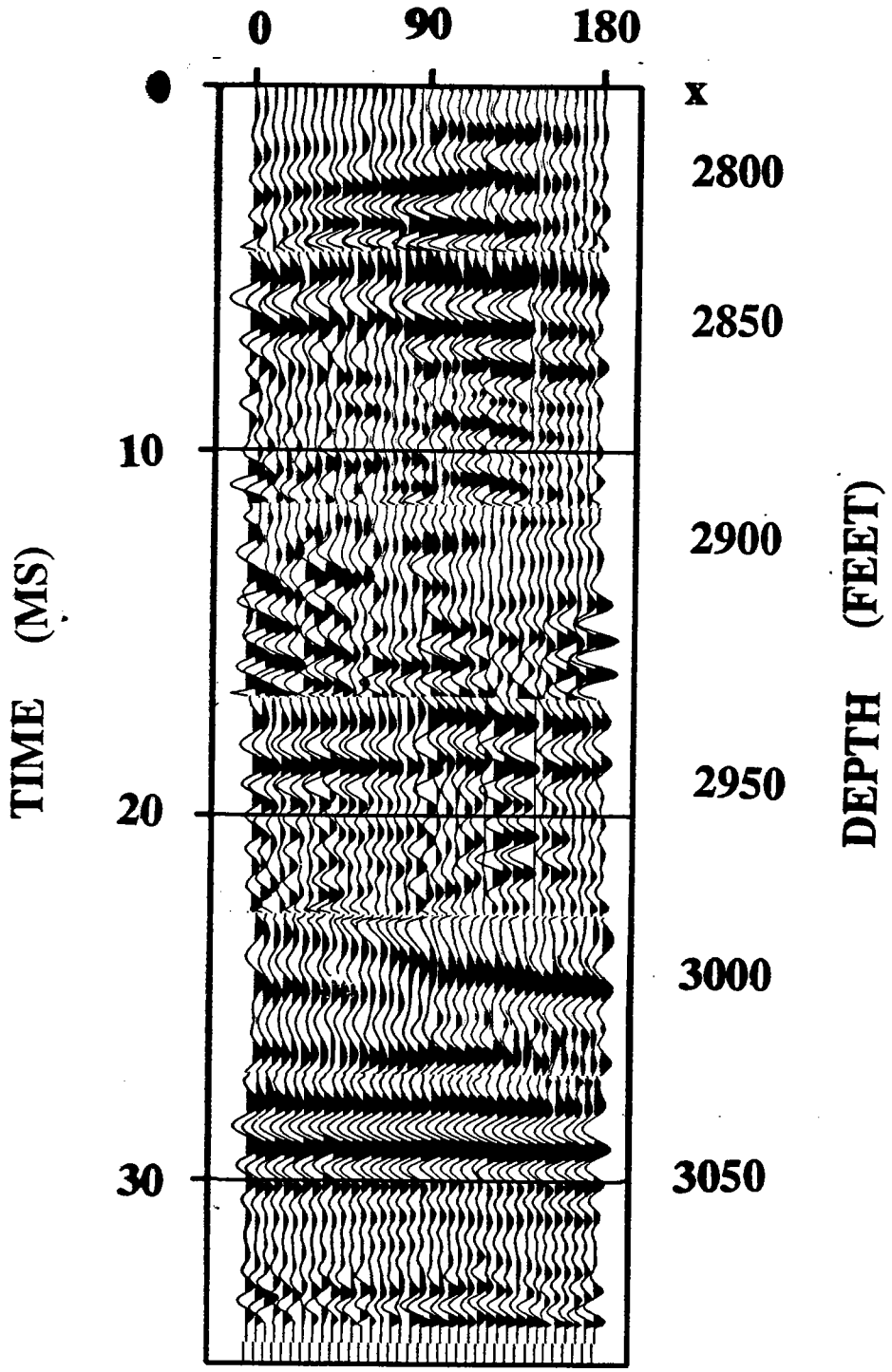

Figure R8. Composite constant velocity reflection image.

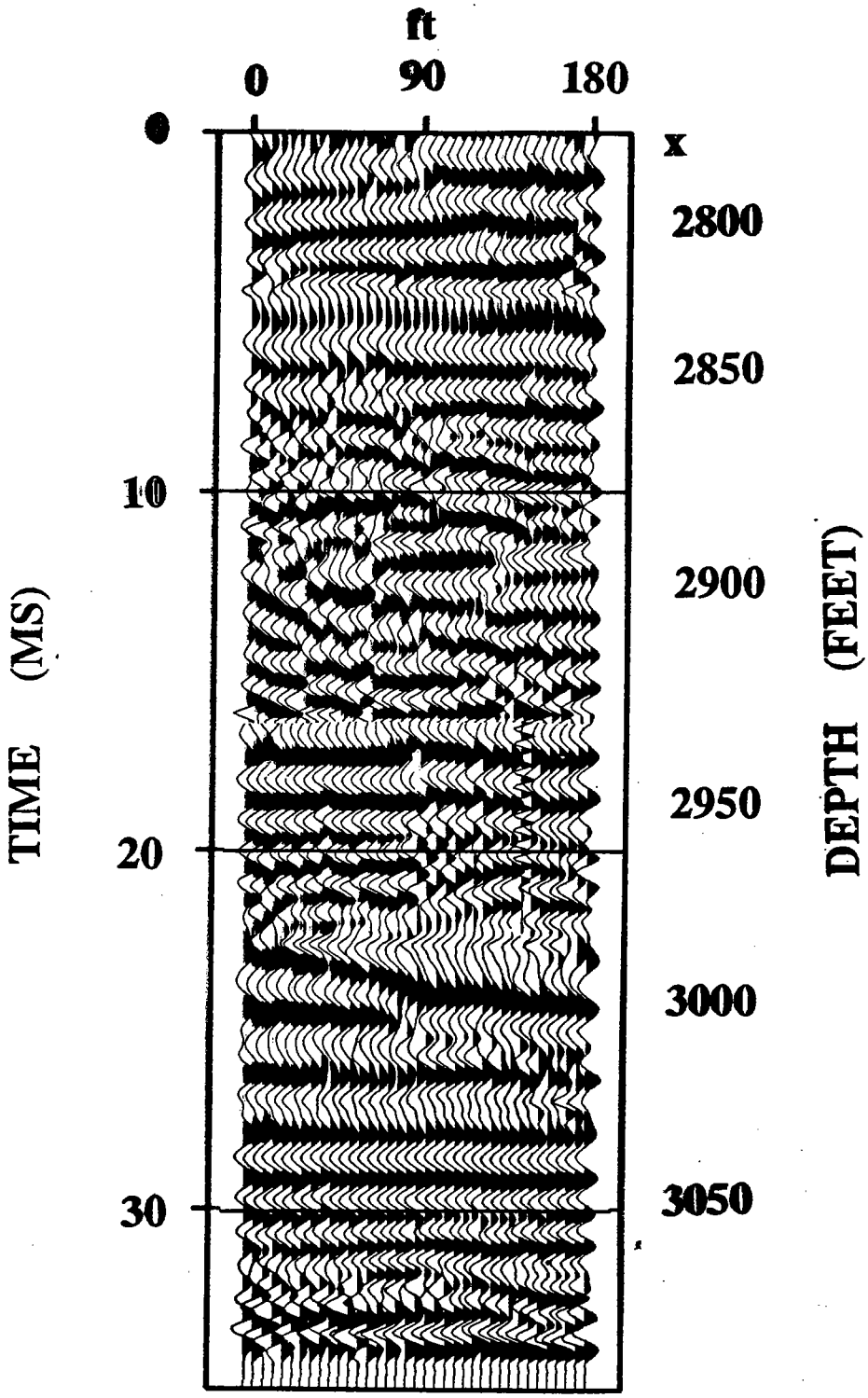

Figure R9. Composite constant velocity reflection image using an AGC window of 3ms.